Soft Matter

Accepted Manuscript

ROYAL SOCIETY OF CHEMISTRY

www.rsc.org/softmatter

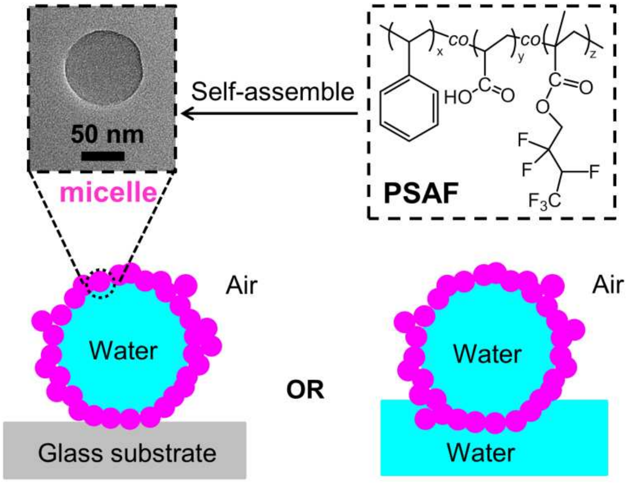

The amphiphilic fluorinated micelles based on the self-assembly of poly(styrene-*co*-acrylic acid-*co*-2,2,3,4,4,4-hexafluorobutyl methacrylate) (PSAF) are prepared and employed as stabilizers to form liquid marbles.

Liquid marbles prepared from pH-responsive self-assembled micelles

Jianhua Sun , Wei Wei, Donghua Zhao, Qiong Hu, Xiaoya Liu *

Key Laboratory of Food Colloids and Biotechnology, Ministry of Education, School of Chemical and Material Engineering, Jiangnan University, Wuxi 214122, China

Abstract

In this study, we reported the assembly of amphiphilic polymeric micelles at the liquid/air interface to prepare liquid marbles for the first time. The polymeric micelles were synthesized from the self-assembly of fluoropolymer, poly(styrene-*co*-acrylic acid-*co*-2,2,3,4,4,4-hexafluorobutyl methacrylate), in a selective solvent. The particle size, morphology and chemical composition of the micelles were determined by dynamic light scattering (DLS), transmission electron microscopy, scanning electron microscopy and X-ray photoelectron spectroscopy. DLS and aqueous electrophoresis revealed the pH-responsiveness of the micelles in aqueous dispersion. The liquid marbles with water volumes varying from 10 μL to 1 mL were formed by rolling water droplets on the micelle powder bed. The increase in water volume could lead to the shape transition of the liquid marbles from quasi-spherical to puddle-like shape because of gravity. Fluorescence microscopy was used to observe the morphology of the formed liquid marbles, which confirmed that the micelles were adsorbed at the interface of water and air. The effective surface tension of the liquid marble decreased with the increasing concentration of NaOH added in the interior water phase. It agreed with the results of droplet roller experiments: the mechanical integrity of the liquid marbles prepared from alkaline solution (pH 10) was relative poorer than those prepared from acidic solution (pH 2). Moreover, these liquid marbles coated with micelles showed pH-responsiveness when transferred onto the surface of water with different pH values. The liquid marbles were relative stable on the acid water, while burst immediately on the alkaline water with pH of 10. In addition, apart from water,

the Gellan gum solution and glycerol could be also successfully encapsulated by the fluorinated micelles to form stable liquid marbles.

Introduction

Liquid marbles, [1] which are prepared through the encapsulation of liquid droplets by adsorbed particles at the liquid/gas interface , have attracted increasing attention due to their potential uses in cosmetics, home and personal care products, [2-3] pollution detection, [4] and microfluidic system. [5] Liquid marbles are usually prepared with relatively hydrophobic particles with the size varying from tens of nanometers to several micrometers. [6-8] Apart from water, some solvent of low vapor pressure such as hexadecane, dimethylsulfoxide, toluene and ethanol, can be encapsulated to form liquid marbles as well.[9]

The stimuli-responsive liquid marbles, which can be stimulated by electric, magnetic fields, UV light or pH, [10-15] have been studied widely. Usually, the responsive ability of the liquid marbles are endowed by the functional “shell”. Much of the examples initially used inorganic particles as the versatile stabilizers, such as carbon black, [16] magnetic particles, [9] and surface-modified titanium dioxide or silica. [17-18] Recently, the organic polymer particles as liquid marble stabilizers have drawn much attention, since they can be readily designed by using various functional monomers. Some sensitive latexes were employed to prepare pH-responsive liquid marbles by Fujii and Armes. [13, 19-20] For example, PS latexes sterically stabilized by poly-[2-(diethylamino) ethyl methacrylate] were used for the preparation of liquid marbles that showed different stability when placed on the surface of water with various pHs. [19] Sun and coworkers utilized the charged PS latexes to study the effect of initial particle state on the responsibilities of the liquid marbles. [21] Also, the thermo-responsive liquid marbles coated with poly(*N*-isopropylacrylamide) (PNIPAM) powder were prepared by Yusa et al..[22] These polymeric particles have shown many advantages in preparing stimuli-responsive liquid marbles, but most of them were synthesized by dispersion polymerization. [13, 19, 21] So, whether the liquid marble stabilizers can be prepared through the way of self-assembly of polymers?

Self-assembly of amphiphilic polymers is an efficient way to prepare versatile polymeric micelles, which is well known for tailoring the structure and surface properties of nanoparticles.[23-25] The properties of the polymeric micelles can be tuned by introducing various functional monomers or changing the method of self-assembly, and the micelles have shown potential applications in many fields including drug delivery, catalysis, and biosensor. [26-28] The assembly behavior of polymeric micelles at oil/water interface was first reported by Fujii et al., who used the shell cross-linked micelles based on the self-assembly of the triblock copolymers to prepare pH-responsive Pickering emulsions. [29] After that, our group also did a lot of work on the study of the interfacial behavior of the polymeric micelles. The polymeric micelles prepared from the self-assembly of random amphiphilic copolymers were surface-active and showed excellent emulsifying performance at the oil/water interface, as reported in our previous study. [30-32] Hence, we guess that the self-assembled micelles based on the random copolymers might be adsorbed at the liquid/gas interface to prepare stimuli-responsive liquid marbles.

Herein, in this study, the fluorinated polymeric micelles based on the self-assembly of fluoropolymers, poly(styrene-*co*-acrylic acid-*co*-2,2,3,4,4,4-

hexafluorobutyl methacrylate), were prepared and further used to stabilize liquid marbles, as shown in Scheme 1. The micelles were characterized by dynamic light scattering (DLS), transmission electron microscopy, and X-ray photoelectron spectroscopy. The pH-responsiveness of the micelles was studied by the method of DLS and aqueous electrophoresis. Moreover, the static properties and mechanical property of the formed liquid marbles were studied, and the morphology of the liquid marbles was observed by fluorescence microscopy. Additionally, these liquid marbles showed pH-responsiveness due to the carboxyl groups in micelles.

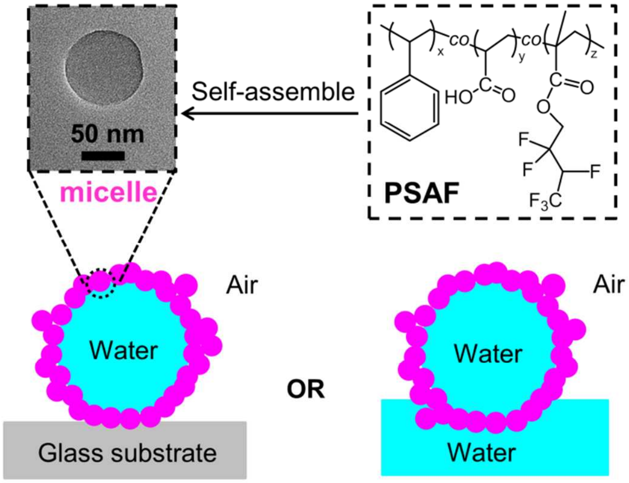

Scheme 1. The amphiphilic fluorinated micelles based on the self-assembly of poly(styrene-*co*-acrylic acid-*co*-2,2,3,4,4,4-hexafluorobutyl methacrylate) (PSAF) are prepared and employed as stabilizers to form liquid marbles.

Experimental section

2.1 Materials. Polymer poly(styrene-*co*-acrylic acid-*co*-2,2,3,4,4,4-hexafluorobutyl methacrylate) (PSAF, Mn=1.21×10^4) were synthesized and characterized as described in details in the *Supplementary Material*. Fluorescein sodium was provided by

Shanghai Chemicals. Rhodamine B and fluorescein sodium were supplied by J&K Scientific Ltd.. Gellan gum was kindly donated by Longjin Bio-Technique Co. Ltd. (LTD, Anhui, China). The water used in all experiments (18.2 MΩ·cm) was purified using a Millipore water purification system.

2.2 Preparation of PSAF self-assembled micelles. The copolymer was dissolved into DMF with the concentration of 20 mg·mL^{-1}, and the solution was stirred overnight. Water was added dropwise into the copolymer solution slowly until the water content reached 0.19 vol.%. The mixture was stirred subsequently for 3 h and then quenched into an excess amount of water, followed by dialysis against water to remove any remaining DMF. To obtain the micelle powder, the micelle aqueous dispersion was dried through freeze-drying under vacuum. In addition, to study the self-assembly process of PSAF, UV–vis spectrophotometry (TU-1901, Beijing Persee Co. Ltd.) was used to detect the turbidity change of the PSAF copolymer in DMF solution.

2.3 Characterization of PSAF micelles. *Particle Size and Zeta Potential.* The Dynamic light scattering (DLS) was carried out using the ALV-5000 laser light scattering spectrometer to size the PSAF micelles, which was operated with a fixed scattering angle of 90° at 25 °C. The micelle aqueous dispersion was filtered through 0.45 μm Millipore filter before test. The average diameter and zeta potential of PSAF micelles against pH were determined with a combination BIC 90Plus and ZetaPALS instrument (Brookhaven Instruments Corp., USA). The concentration of the micelle aqueous dispersions was 0.5 mg mL^{-1} with 0.01 mM NaCl.

Transmission Electron Microscopy (TEM). The TEM observation of the PSAF micelles was obtained using a JEOL JEM-2100 (HR) LaB6 transmission electron microscope operating at an accelerating voltage of 200 kV. The samples were prepared by dropping diluted PSAF micelle aqueous dispersions onto the carbon-coated copper grid and then drying at room temperature overnight.

Scanning electron microscopy (SEM). The SEM studies were conducted on a Quanta-200 field-emission microscope operated at an accelerating voltage of 20 kV. The dried micelles were placed on a copper stub and sputter coated with thin layer of gold prior to examination to minimize sample-charging problems.

X-ray Photoelectron Spectroscopic Study. The X-ray photoelectron spectroscopy (XPS) measurement was carried on a ESCALAB 250 photoelectron spectrometer (Thermo-VG Scientific, America) equipped with a microfocused monochromatic Al Kα X-ray source (1486.6 eV). The survey spectra were recorded using pass energy of 30 eV at 90°take off angle. The C 1s XPS spectrum was peak-fitted with the XPSPEAK software, Version 4.1.

Contact Angle Measurement. For the contact angles measurement, sessile drop technique was used. The water droplets with pH of 2 and 10 were dripped on the PSAF micelle powder sheets, and the contact angle was measured by an OCA15EC contact angle measurement instrument (Dataphysics Ltd., German).

2.4 Preparation of Liquid Marbles. The Liquid marbles were formed by rolling water droplets onto the PSAF micelle powder bed using a micropipette. The volume of the dispensed water droplet was varied from 10 μL to 1mL.

2.5 Characterization of Liquid Marbles. *Fluorescence Microscopy.* The Droplets of 40 μL of an aqueous solution containing 2.0 wt % Gellan gum and 0.01 wt % fluorescein sodium at 60 ^{o}C were encapsulated by Rhodamine B labeled-PSAF micelles to prepare liquid marbles. After cooling to room temperature, the droplet phase was gelled, then the liquid marble was solidified. To observe the micelles adsorbed at the interface directly, the solidified liquid marble was cut in half and observed with a Nikon 80i fluorescence microscopy (Nikon Co., Ltd., Japan). The fluorescence excited wavelength for fluorescein sodium and Rhodamine B were 465~495 nm and 540~565 nm respectively.

2.6 Mechanical property of liquid marbles. In order to investigate the mechanical integrity of liquid marbles, the droplet roller experiments were carried out. The illustration of the home-made apparatus was shown in Fig. S4 in the *Supplementary Information*. The "runway" for the droplets was overspread with PSAF micelle powder with a fixed inclination angle of 20^{o}. 10 μL of water droplets containing Rhodamine B were dripped on the runway, the liquid marbles were formed after rolling on the micelle powder bed. The height between the slop and the substrate (with micelle powder bed or not) was varied from 0 to 9 cm to investigate the mechanical property of the liquid marbles. 20 liquid marbles were examined for each height, 10 droplets were dripped on the substrate with micelle powder bed, and 10 droplets were directly dripped on the bare substrate.

Results and discussion

3.1 Self-assembly of PSAF.

The micelles based on PSAF were formed in a selective solvent. In order to study the self-assembly behavior of PSAF in the selective solvent, the turbidity of the polymer solution was traced by UV–vis spectrophotometry when adding water into the polymer solution in DMF, as shown in Fig. S3. The turbidity increases dramatically as the water content reaches 11 vol% where is defined as critical water content (CWC). This point of CWC indicates that the polymer segments start to aggregate. When the turbidity reaches a plateau, it suggests that the stable micelles are formed.

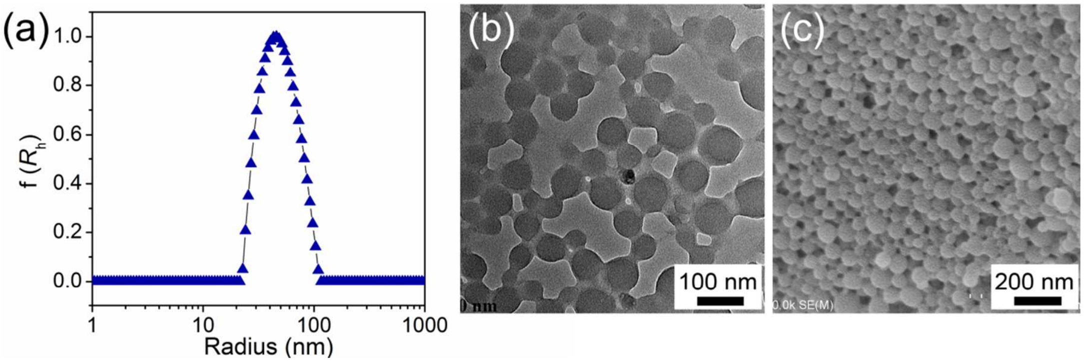

Fig. 1 (a) Radius of PSAF micelles determined by DLS.

(b) TEM image of PSAF micelles. (c) SEM image of PSAF micelle powder.

The size of PSAF micelles in aqueous dispersion was determined by DLS, and the analysis indicates a narrow size distribution of the micelles with the average diameter of 192 nm (see Fig. 1a).The spherical morphology of micelles was confirmed by TEM, as shown in Fig. 1b. The diameter of the dried micelles of about 80 nm is smaller than that measured by DLS, which is because that the micelles are swollen with water in the aqueous dispersion. A typical SEM image of the dried micelle powder is shown in Fig. 1c. A relatively monodisperse, spherical morphology can be observed, which agrees well with the TEM image.

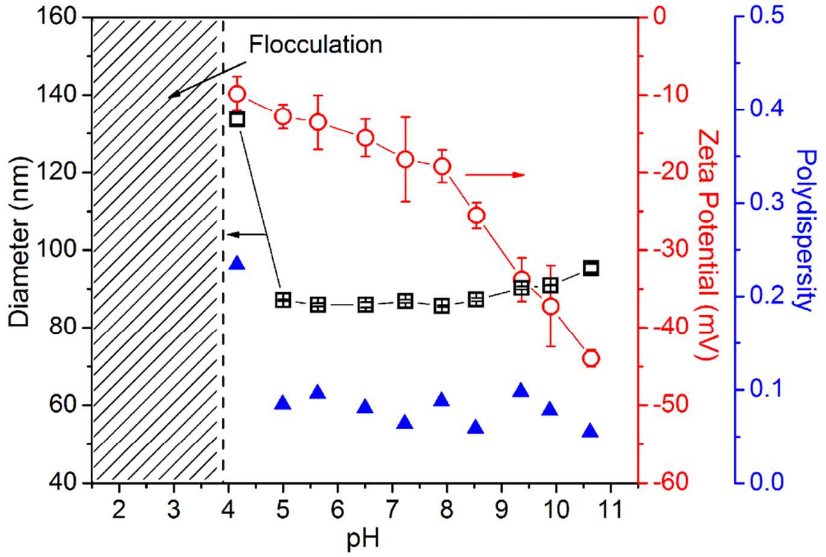

Fig. 2 Effect of pH on the diameter, zeta potential and polydispersity of PSAF micelles. The concentration of micelle dispersion is 0.5 mg·mL^{-1} with 0.01M NaCl. Note that, the error bar of the diameter is too small to be shown.

The pH-sensitivity of PSAF micelles was monitored using DLS and aqueous electrophoresis. The values of zeta potential, hydrodynamic diameter and polydispersity of the micelles are plotted against the pH of the aqueous dispersion in Fig. 2. The zeta potential increases from -9 mV to -44 mV with increasing pH values. It is mainly due to the deprotonation of the carboxylic acid groups. The hydrodynamic diameter of the micelles changes less at pH>5, the increase in diameter from 87 nm to 95 nm can be attributed to the electrostatic repulsion force among the polymer chains in the micelles, which suggests that the PSAF micelles have a stable structure. Note that the micelle size increases at pH 4, and the micelles are too flocculated to allow to size the diameter when pH<4 (see the shadow area in Fig. 2). Combining the result of zeta potential, the micelles charge less at low pH, the electrostatic repulsion force between the particles reduces, resulting in the aggregation of the particles. The polydispersity of the micelles also increases at pH 4 where the micelles are started to flocculated.

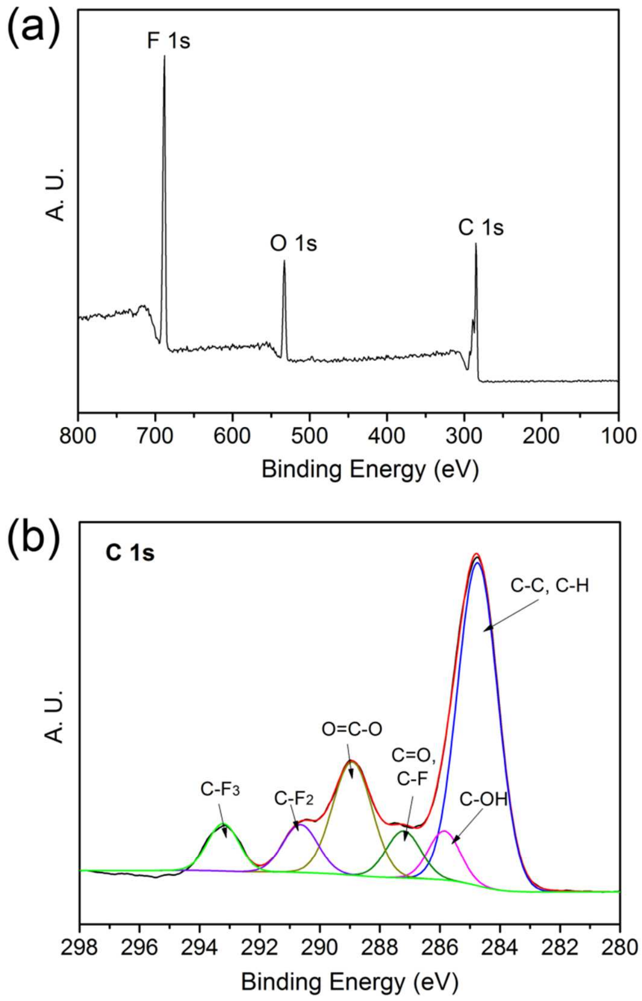

Fig. 3 (a) XPS spectrum of PSAF micelle powder.

(b) XPS C1s spectrum and its fitting curves for PSAF micelle powder.

Fig. 3a shows the XPS spectrum recorded for PSAF micelles, the peaks at binding energies of 688, 532 and 284 eV are attributed to F 1s, O 1s and C 1s, respectively. According to the result calculated by XPS, the composition contents of micelles in term of F, O and C are 32.91%, 14.38% and 52.71 %. In Fig. 3b, the XPS

C1s spectrum of the micelles is fitted with six peaks at 284.6, 285.8, 287.5, 288.9, 290.6, and 293.1 eV corresponding to the following groups: C-C or C-H (aromatic and aliphatic carbon), C-OH, C=O or C-F, O=C-O(carboxyl or ester), C-F_2 and C-F_3, respectively. Given that the XPS survey typically detects the surficial chemical composition of materials, these observations provide an evidence that the hydrophobic and hydrophilic units coexist on the surface of PSAF micelles, indicating that the micelles are amphiphilic. This result also conforms to the theory of self-assembly of amphiphilic random copolymers.[33]

3.2 Preparation of liquid marbles

The liquid marbles were formed by rolling water droplets on the PSAF micelle powder bed. The nanoparticles can spontaneously self-organized at the droplet surface, which is attributed to the minimization of the surface free energy. [1, 34]

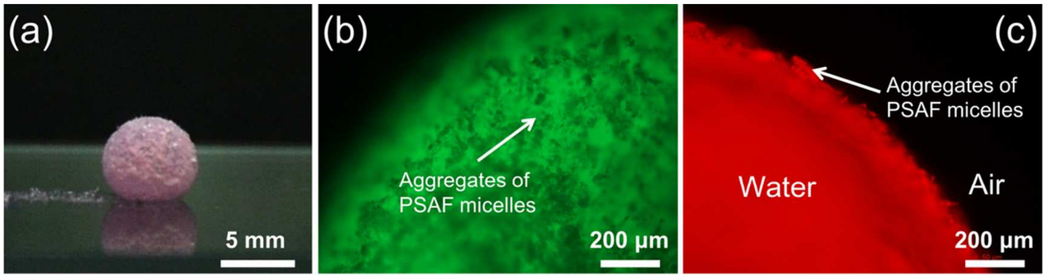

Fig. 4 (a) Digital photographs of the liquid marble prepared from Rhodamine B-labeled PSAF micelle powder. (b) Fluorescence microscopic images of solidified liquid marbles with the excitation wave band of 465~495 nm. The fluorescein sodium in the internal phase was excited. The green region is the internal phase, and the dark blocks are the aggregates of PSAF micelles. (c) Fluorescence microscopic images of the section of solidified liquid marbles with the excitation wave band of 540~565 nm. The Rhodamine B-labeled PSAF micelle are adsorbed at the surface of the section, and the emitting light of Rhodamine B makes the whole section appear red. The red

blocks at the out layer are the aggregates of PSAF micelles.

The liquid marbles covered with PSAF micelles are unstable on the glass substrate, they collapse gradually due to the evaporation of water from interior. In order to observe the micelles adsorbed at the liquid/air interface directly, Gellan gum aqueous solution was used as the liquid phase. The liquid marbles were prepared with a 2.0% Gellan gum aqueous solution containing 0.01 wt % fluorescein sodium at 60 ^{o}C and the Rhodamine B labeled-PSAF micelles. When the Gellan gum liquid marble cooled to room temperature, the whole marble was solidified. Fig. 4a shows the photograph of the liquid marble stabilized by Rhodamine B-labeled PSAF micelles on a glass substrate.

The surface morphology of the liquid marble was observed with the excitation wave band of 465~495 nm (fluorescein sodium was excited), as shown in Fig. 4b. The green region is the internal phase of the liquid marble, and the dark particles are the aggregates of PSAF micelles that adsorbed at the surface. Fig. 4c shows the fluorescence microscopic images of the section of the liquid marble with the excitation wave band of 540~565 nm which can excite Rhodamine B. The red blocks at the edge of section are the aggregates of Rhodamine B labeled-PSAF micelles. However, the internal phase appears red as well. It is because that the surface of the liquid marble section is all covered by Rhodamine B labeled-PSAF micelles, and the emitting light of the Rhodamine B passes through the transparent internal phase.

The relationship between the shape of a liquid marble and the water volume was studied, as shown in Fig. 5. Parameters a, b and c were used to define the diameter of the contact area between liquid marble and the glass substrate, height and horizontal diameter of the liquid marble, respectively (see the insert in Fig. 5). The solid curve indicates the diameter (b') of the water droplets with a perfectly spherical morphology against water volume, which is assumed that the shape of water droplet is independent of water volume. The liquid marbles take an almost spherical shape for small volumes, but deform strongly as the volume increases with a puddle shape. The deviation of the dimension of the liquid marbles from the theoretical values expected for a sphere becomes large with the increase in water volume, which is caused by the gravitational force. The maximum height ($H_{\max}$) of the liquid marble is related to the capillary length (κ^{-1}) [35]:

$$\kappa^{-1} = \sqrt{\frac{\gamma}{\rho g}} \qquad (1)$$

Where γ is the effective surface tension of the liquid marble, ρ is the water density ($1.00\ \mathrm{g\cdot cm^{-1}}$), and g is the acceleration due to gravity ($9.81\ \mathrm{m\cdot s^{-1}}$). The effective surface tension (γ) can be calculated from: [36]

$$\gamma = \frac{\rho g {H_{\max}}^{2}}{4} \qquad (2)$$

Based on the results shown in Fig. 5, the $H_{\max}$ of the liquid marbles is estimated to be 5.2 mm, κ^{-1} is calculated from eq 1with the value of 2.6 mm. The effective surface tension (γ) is calculated to be 66 $\mathrm{mN\cdot m^{-1}}$ by use of eq 2. Compared with pure water (γ = 72 $\mathrm{mN\cdot m^{-1}}$), the reduction in the effective surface tension can be attributed to the hydrophobic PSAF micelles coating on the water droplet surface. In principle, if the quasi-spherical radius (R_0) of water droplet is much larger than κ^{-1}, the droplets take a puddle shape due to gravity. [37] Here, $R_0 = (3V/4\pi)^{1/3}$, where V is the water volume. In our case, the liquid marbles with the volume of 10~20 μL (R_0 =1.3~1.7 mm) have a near-spherical shape, and the larger liquid marbles (> 100μL) are considered to be in puddle-like shape, shown in Fig. 5.

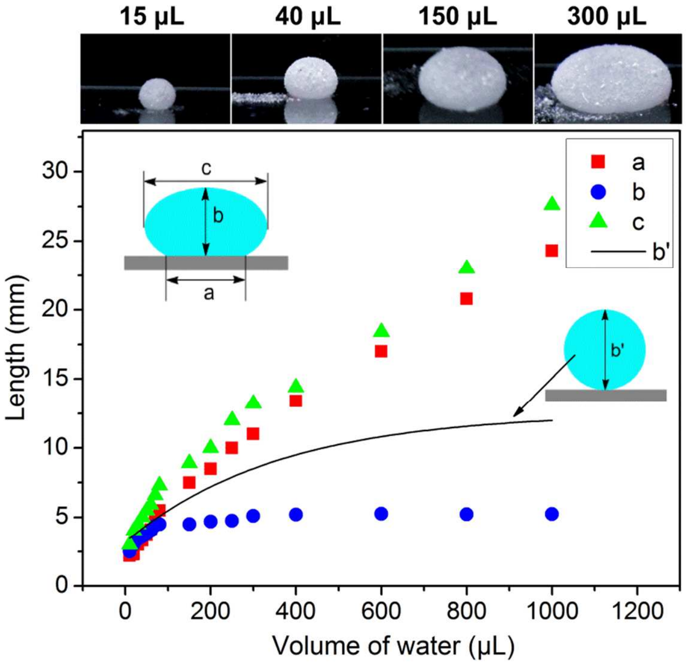

Fig. 5 Relationship of the diameter of the contact area, height, and width of the liquid marbles with water volume. The solid curve is the theoretical diameter of a quasi-spherical droplet with various water volumes.

The ratio of horizontal diameter (c) over the height of the liquid marble (b) at different pH values of the internal liquid phase was calculated, as shown in Fig. 6. The ratio increases with the increasing concentration of NaOH added in the water, which indicates the gradual collapse of the liquid marble. This phenomenon should be attributed to the improved hydrophility of the micelles which caused by the deprotonation of the micelles. The effective surface forces of the liquid marble covered by the hydrophilic micelles reduces and cannot hold the weight of the water droplet to maintain its spherical form. [21] In the higher concentration of NaOH, the micelles were fully incorporated into the aqueous phase, the liquid marbles could not be formed.

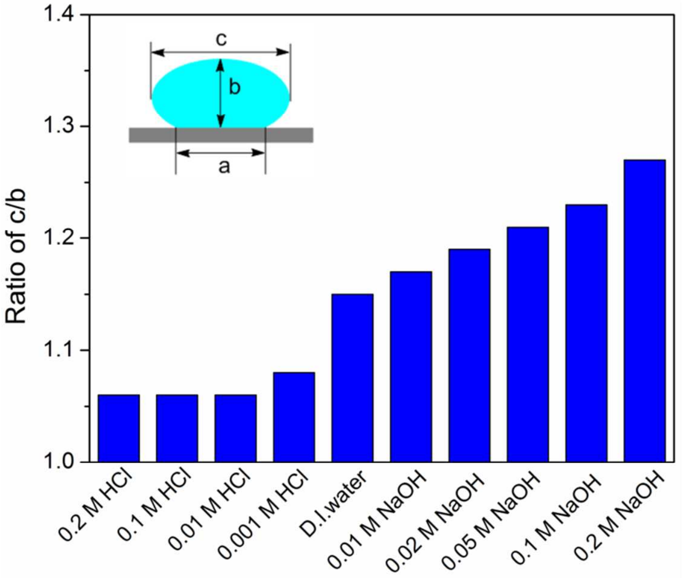

Fig. 6 Effect of the concentration of NaOH added in the water droplet on the shape evolutions of liquid marbles stabilized by PSAF micelles. The volume of the droplet is 15μL.

The mechanical integrity of the liquid marbles prepared from different aqueous solution pH was investigated by the droplet roller experiments, as shown in Table 1. At pH 2, the liquid marbles were intact and kept a spherical shape with their original water volume when rolling from the height of 2 cm or lower (with micelle powder bed or not, shown in Fig. 7 a and d). Between the height of 3 to 5 cm, the liquid marbles were broken immediately if there was no micelle powder on the substrate. While, if the liquid marbles crashed on the micelle powder bed, they deformed without disintegration. Above a height of 5 cm, only on the micelle powder bed can the liquid marbles survive, with one big deformed droplet and several small ones separated from the "parent" liquid marble (see Fig. 7c). The impinging kinetic energy

(E_i) per liquid marble (10 μL) for the experiments conducted at a height of 5 cm was estimated to 5.0×10^{-6} J. E_i is 3.5 times larger than the liquid marble surface energy (E_s) of 1.4×10^{-6} J which is calculated by combining the effective surface tension (66 $mN\cdot m^{-1}$) and water volume (10 μL). The mechanical property of liquid marbles at pH 10 was relatively poor compared with that at solution pH of 2. The liquid marbles broke up even at the rolling height of 1 cm when there was no powder bed, and their deformation was found just at a height of 2 cm on the powder. Agreed with the results in Fig. 6, the hydrophility of the PSAF micelles is improved at high pH value, the micelles cannot be adsorbed at the water/air interface effectively, leading to the unstableness of the liquid marbles.

Table. 1 Characterization of mechanical integrity of liquid marbles stabilized by PSAF micelle powder.

	pH 2[a]		pH 2[b]		pH 10[a]		pH 10[b]	
height (cm)	rolling (%)	deformed (%)	rolling (%)	broken (%)	rolling (%)	deformed (%)	rolling (%)	broken (%)
0	100	0	100	0	100	0	100	0
1	100	0	100	0	100	0	0	100
2	100	0	100	0	90	10	0	100
3	90	10	0	100	90	10	0	100
4	90	10	0	100	50	50	0	100
5	60	40	0	100	0	100	0	100
6	0	100	0	100	0	100	0	100
7	0	100	0	100	0	100	0	100
8	0	100	0	100	0	100	0	100
9	0	100	0	100	0	100	0	100

[a] The liquid marbles were dripped onto the powder bed. [b] The liquid marbles were dripped onto the bare substrate.

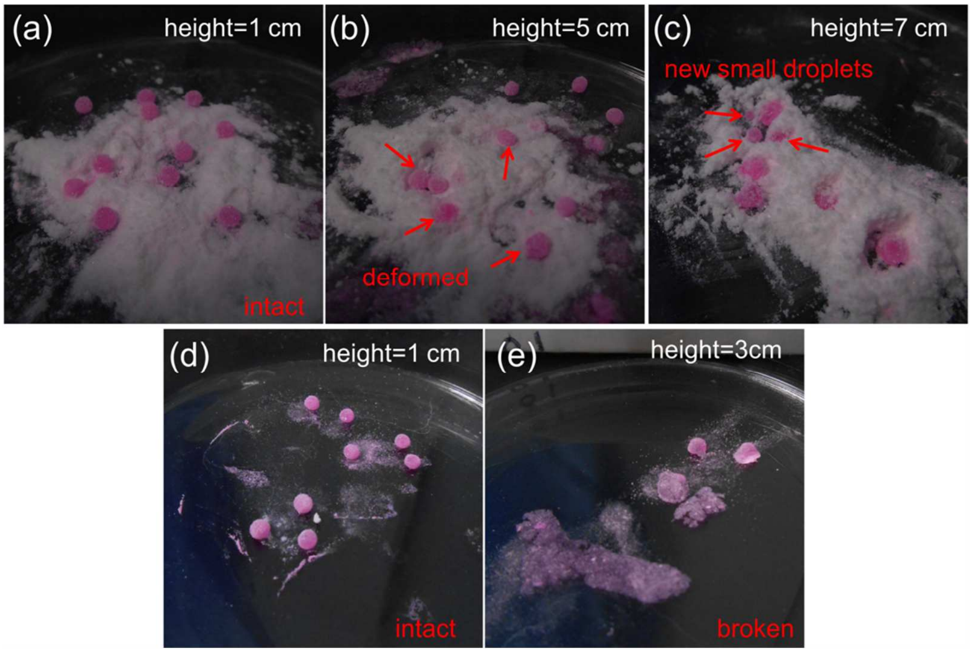

Fig. 7 Digital pictures of liquid marbles stabilized by PSAF micelle powder rolling from different heights. (a)-(c) dripped onto the micelle powder bed; (d)-(e) dripped onto the bare substrate. The water volume for the liquid marble is 10 μL.

In principle, liquid marbles can display non-adhesive and non-wetting behavior towards many surfaces. In our case, the liquid marbles stabilized by PSAF micelles could be transferred onto the surface of water as well. The micelles coating at the droplet surface play an important role to prevent the diffusion of water between the droplet interior and the aqueous subphase. In order to investigate the pH-responsive nature of the liquid marbles prepared by PSAF micelles, these liquid marbles were transferred onto the surface of water with various pH values. As expected, the liquid marbles placed onto the acid water relative are stable than that placed onto the basic water, as shown in Fig. 8. The longest mean lifetime of 425 s was observed at pH 2. At this pH value, the micelles are very hydrophobic due to the almost complete protonation of the carboxyl groups, and the hydrophobic micelles can be strongly adsorbed at the interface to stabilize the liquid marble. When the solution pH is elevated, the micelles contacting with water tend to be incorporated into the solution, leading to a breach in the original intact barrier. The micelle barrier can be destroyed much more easily with the increasing of pH value. At pH 10, the liquid marbles burst immediately when transferred onto the alkaline solution. Further, to confirm the effect of pH on the wettability of the micelles, the contact angle measurement was carried out (see the insert in Fig. 8). The contact angle of 105±2 ° at pH 2 is larger than that of 66±3 ° at pH 10, indicating that the wettability transition of PSAF micelles varies from hydrophobicity to hydrophilicity as the pH of the water increases.

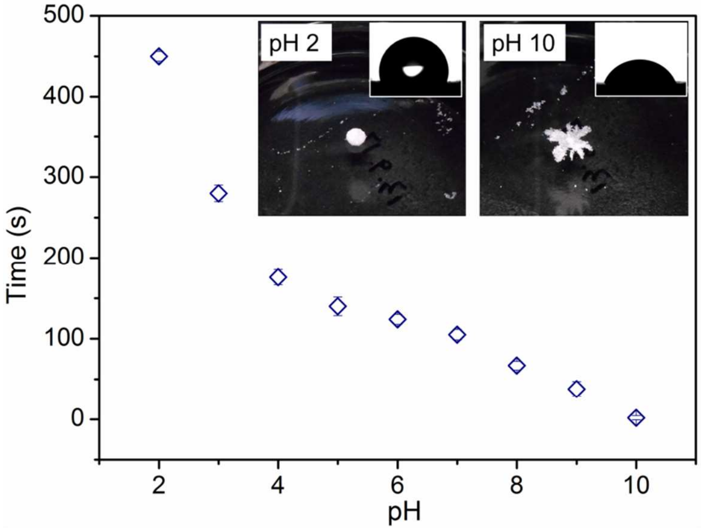

Fig. 8 Mean lifetime of liquid marbles (15μL) prepared from PSAF micelle powder after being transferred on the surface of water with various pH values.

The encapsulated liquid of liquid marbles can be aqueous solution or the solvent of low vapor pressure. Xue et al. reported the liquid marbles prepared from fluorinated decyl polyhedral oligomeric silsesquioxane in combination with hydrophobic magnetic nanoparticles to encapsulate some organic liquids of low surface tension. [9] In general, the particles with the property of superior oil repellence are capable to stabilize oil droplets. In this study, apart from water and the Gellan gum solution, glycerol liquid marbles were prepared successfully by use of PSAF micelle powder, as shown in Fig. 9. The glycerol marbles adopted a spherical shape on a glass substrate. In addition, the 40 μL glycerol liquid marbles can float at the surface of liquid water even if the density of glycerol (1.26 g·cm^{-3}) is higher than that of water, which is governed by the interplay between surface tension and gravity. [35]

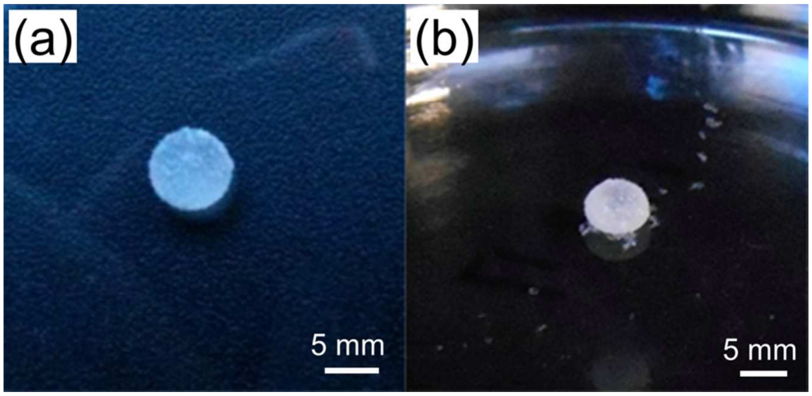

Fig. 9 Digital photographs of a glycerol liquid marble stabilized with PSAF micelle powder. This droplet is placed on a glass substrate (a) and at the surface of water (b).

Conclusions

In this study, the fluorinated PSAF micelles were successfully prepared from the self-assembly of pH-responsive PSAF fluoropolymers. The spherical morphology of the micelles was confirmed by means of TEM and SEM. These micelles showed pH-responsiveness due to the carboxyl groups in copolymers. The zeta potential increased from -9 mV to -44 mV , and the micelle size increased from 87 nm to 95 nm as the pH value was elevated. Moreover, the PSAF micelles were used to prepare liquid marbles. The morphology of the formed liquid marbles was observed by fluorescence microscopy, suggesting that the micelles were adsorbed at the interface of water and air. The water volumes of the liquid marbles stabilized with PSAF micelles could vary from 15 μL to 1mL. The larger liquid marbles adopted a puddle-like shape because of gravity. Also, the addition of NaOH in the inner water could undermine the shape of liquid marbles, which is due to the deprotonation of the micelles in the alkaline condition. The mechanical integrity of the liquid marbles was studied by the droplet roller experiments, the results showed that the liquid marbles prepared from acidic aqueous solution (pH 2) was relatively stable than those prepared from alkaline aqueous solution (pH 10). Additionally, these liquid marbles coated with the PSAF micelles showed pH-responsiveness when transferred onto the surface of water with various pH values. Liquid marbles were relative stable when the pH values of subphase was low. While the immediate disintegration of liquid marbles was found at pH 10. Apart from water, Gellan gum solution and glycerol were also successfully encapsulated by the PSAF micelles to form stable liquid marbles.

Acknowledgements

We acknowledge financial support from the National Nature Science Foundation of China (Grant no. 20974041, B0405), the Fundamental Research Funds for the Central Universities (JUSRP 51305A), and MOE & SAFEA for the 111 Project (B13025).

Notes and references

The Key Laboratory of Food Colloids and Biotechnology, Ministry of Education, School of Chemical and Material Engineering, Jiangnan University, Wuxi, Jiangsu 214122, P. R. China

*Corresponding author: Fax: 86-510-85917763; Tel: 86-510-85917763; E-mail: lxy@jiangnan.edu.cn

Electronic Supplementary Information (ESI) available: The synthesis of PSAF polymers; the FTIR characterization of PSAF; the self-assembly process traced by UV. See DOI: 10.1039/b000000x/

1 P. Aussillous and D. Quere, *Nature*, 2001, **411,** 924-927.

2 K. M. Lahanas, N. Vrabie, E. Santos and S. Miklean, *US Pat.*, 6 290 941, 2001.

3 C. Dampeirou, *WO Pat.*, 034 917, 2005.

4 M. D. Hoffman and I. L. Chiu, *US Pat.*, 7 030 071, 2006.

5 J. R. Dorvee, A. M. Derfus, S. N. Bhatia and M. J. Sailor, *Nat Mater*, 2004, **3,** 896-899.

6 E. Bormashenko, R. Pogreb, G. Whyman, A. Musin, Y. Bormashenko and Z. Barkay, *Langmuir*, 2009, **25,** 1893-1896.

7 N. Eshtiaghi, J. J. S. Liu and K. P. Hapgood, *Powder Technol*, 2010, **197,** 184-195.

8 W. X. Wang, C. L. Bray, D. J. Adams and A. I. Cooper, *J Am Chem Soc*, 2008, **130,** 11608-+.

9 Y. H. Xue, H. X. Wang, Y. Zhao, L. M. Dai, L. F. Feng, X. G. Wang and T. Lin, *Adv Mater*, 2010, **22,** 4814-+.

10 Y. Zhao, Z. G. Xu, M. Parhizkar, J. Fang, X. G. Wang and T. Lin, *Microfluid Nanofluid*, 2012, **13,** 555-564.

11 Y. H. Xue, H. X. Wang, Y. Zhao, L. M. Dai, L. F. Feng, X. G. Wang and T. Lin, *Adv Mater*, 2010, **22,** 4814-4818.

12 K. Nakai, S. Fujii, Y. Nakamura and S. Yusa, *Chem Lett*, 2013, **42,** 586-588.

13 S. Fujii, S. Kameyama, S. P. Armes, D. Dupin, M. Suzaki and Y. Nakamura, *Soft Matter*, 2010, **6,** 635-640.

14 D. Dupin, S. P. Armes and S. Fujii, *J Am Chem Soc*, 2009, **131,** 5386-+.

15 K. Nakai, H. Nakagawa, K. Kuroda, S. Fujii, Y. Nakamura and S. Yusa, *Chem Lett*, 2013, **42,** 719-721.

16 E. Bormashenko, Y. Bormashenko, R. Pogreb and O. Gendelman, *Langmuir*, 2011, **27,** 7-10.

17 Z. G. Xu, Y. Zhao, L. M. Dai and T. Lin, *Part Part Syst Char*, 2014, **31,** 839-842.

18 T. T. Y. Tan, A. Ahsan, M. R. Reithofer, S. W. Tay, S. Y. Tan, T. S. A. Hor, J. M. Chin, B. K. J. Chew and X. B. Wang, *Langmuir*, 2014, **30,** 3448-3454.

19 S. Fujii, M. Suzaki, S. P. Armes, D. Dupin, S. Hamasaki, K. Aono and Y. Nakamura, *Langmuir*, 2011, **27,** 8067-8074.

20 K. Ueno, S. Hamasaki, E. J. Wanless, Y. Nakamura and S. Fujii, *Langmuir*, 2014, **30,** 3051-3059.

21 G. Q. Sun, Y. F. Sheng, J. Wu, G. H. Ma and T. Ngai, *Langmuir*, 2014, **30,** 12503-12508.

22 S. Yusa, M. Morihara, K. Nakai, S. Fujii, Y. Nakamura, A. Maruyama and N. Shimada, *Polym J*, 2014, **46,** 145-148.

23 X. Y. Liu, J. S. Kim, J. Wu and A. Eisenberg, *Macromolecules*, 2005, **38,**

6749-6751.

24 Y. H. Deng, Y. B. Li and X. G. Wang, *Macromolecules*, 2006, **39,** 6590-6598.

25 Y. Y. Mai and A. Eisenberg, *Chem Soc Rev*, 2012, **41,** 5969-5985.

26 J. J. Du, X. Guo, J. X. Tu, L. Q. Xiao, X. X. Jia, L. Q. Liao and L. J. Liu, *Carbohyd Polym*, 2012, **90,** 569-574.

27 K. Y. Sui, X. Zhao, Z. M. Wu, Y. Z. Xia, H. C. Liang and Y. J. Li, *Langmuir*, 2012, **28,** 153-160.

28 O. Bertrand, C. A. Fustin and J. F. Gohy, *Acs Macro Lett*, 2012, **1,** 949-953.

29 S. Fujii, Y. L. Cai, J. V. M. Weaver and S. P. Armes, *J Am Chem Soc*, 2005, **127,** 7304-7305.

30 C. L. Yi, Y. Q. Yang, Y. Zhu, N. Liu, X. Y. Liu, J. Luo and M. Jiang, *Langmuir*, 2012, **28,** 9211-9222.

31 X. Y. Liu, C. L. Yi, Y. Zhu, Y. Q. Yang, J. Q. Jiang, Z. G. Cui and M. Jiang, *J Colloid Interf Sci*, 2010, **351,** 315-322.

32 C. L. Yi, J. H. Sun, D. H. Zhao, Q. Hu, X. Y. Liu and M. Jiang, *Langmuir*, 2014, **30,** 6669-6677.

33 Y. B. Li, Y. H. Deng, X. L. Tong and X. G. Wang, *Macromolecules*, 2006, **39,** 1108-1115.

34 G. McHale, N. J. Shirtcliffe, M. I. Newton, F. B. Pyatt and S. H. Doerr, *Applied Physics Letters*, 2007, DOI: 10.1063/1.2435594.

35 E. Bormashenko, Y. Bormashenko and A. Musin, *J Colloid Interf Sci*, 2009, **333,** 419-421.

36 E. Bormashenko, R. Pogreb, G. Whyman and A. Musin, *Colloid Surface A*, 2009, **351,** 78-82.

37 D. Quere and P. Aussillous, *Chem Eng Technol*, 2002, **25,** 925-928.